Eye (2011) 25, 261–267

www.nature.com/eye

CAMBRIDGE OPHTHALMOLOGICAL SYMPOSIUM

Anterior chamber angle imaging with optical coherence tomography

CK-S Leung[1] and RN Weinreb[2]

Abstract

The technology of optical coherence tomography (OCT) has evolved rapidly from time-domain to spectral-domain and swept-source OCT over the recent years. OCT has become an important tool for assessment of the anterior chamber angle and detection of angle closure. Improvement in image resolution and scan speed of OCT has facilitated a more detailed and comprehensive analysis of the anterior chamber angle. It is now possible to examine Schwalbe's line and Schlemm's canal along with the scleral spur. High-speed imaging allows evaluation of the angle in 360°. With three-dimensional reconstruction, visualization of the iris profiles and the angle configurations is enhanced. This article summarizes the development and application of OCT for anterior chamber angle measurement, detection of angle closure, and investigation of the pathophysiology of primary angle closure.
Eye (2011) **25,** 261–267; doi:10.1038/eye.2010.201; published online 14 January 2011

Keywords: anterior chamber angle imaging; optical coherence tomography; swept-source OCT; spectral-domain OCT

Although gonioscopy is an indispensible technique to visualize the angle structures and estimate the angle width, objective and reproducible measurement of the dimensions of the anterior chamber angle can only be obtained with cross-sectional imaging devices from technologies such as ultrasound biomicroscopy (UBM) and optical coherence tomography (OCT). OCT has a number of advantages over UBM for anterior chamber angle imaging. OCT is a non-contact technique, has a higher image resolution, and is more precise in locating the position of interest for evaluation compared with UBM. It is recognized, however, that UBM has a unique role in visualizing the ciliary body. Although early generations of OCT were designed for imaging the macula and the optic disc, commercially available time-domain and spectral-domain models have been developed for anterior segment imaging. Visualization of the anterior chamber angle not only augments the diagnostic performance to detect a narrow angle and angle closure, but also improves our understanding of the pathophysiology of primary angle closure. This article provides an overview and update on the development and application of OCT for anterior chamber angle imaging.

The time-domain OCT

Since the introduction of the prototype in 1991,[1] OCT has become an important tool in diagnosing macular diseases and glaucoma. Yet, only a few studies attempted to evaluate the anterior chamber angle in the 90s. Izatt *et al*[2] reported the use of an OCT with a compact 830 nm superluminescent diode light source mounted on a standard slit-lamp biomicroscopy to image the anterior segment. It took $\sim$6 s to capture an area of 7×4.4 mm with a resolution of 200×500 pixels. Limited by a relatively low-image resolution, the details of the angle structures could not be clearly discerned. The third generation of OCT, the Stratus OCT (Carl Zeiss Meditec, Dublin, CA, USA), was commercially available in 2002. It has a faster scan speed (400 A-scans per s) and a higher axial resolution (10 μm) compared with the early OCT versions, including the prototype OCT, OCT 1 (Carl Zeiss Meditec), and OCT 2000 (Carl Zeiss Meditec). Leung *et al* illustrated the application of the Stratus OCT to investigate the dynamic changes of angle configurations in patients with primary angle closure, plateau iris configuration, and phacomorphic glaucoma.[3] Widening of the angle and flattening of the iris were demonstrated after laser iridotomy and

[1]Department of Ophthalmology and Visual Sciences, Hong Kong Eye Hospital, The Chinese University of Hong Kong, Hong Kong, PR China

[2]Hamilton Glaucoma Center, Department of Ophthalmology, University of California, San Diego, CA, USA

Correspondence: CK-S Leung, Department of Ophthalmology and Visual Sciences, Hong Kong Eye Hospital, The Chinese University of Hong Kong, 147K Argyle Street, Kowloon, Hong Kong
Tel: +825 3408 7911; Fax: +825 2720 3299.
E-mail: tlims00@hotmail.com

Received: 3 November 2010
Accepted in revised form: 12 November 2010
Published online: 14 January 2011

argon laser peripheral iridoplasty (Figure 1a and b). Similar observation was subsequently reported with other OCT systems specifically designed for anterior segment imaging.[4–6] Although the configuration of the peripheral iris in relation to scleral–corneal junction could be examined with the Stratus OCT, the scleral spur, an anatomical landmark for measurement of the angle width and evaluation of angle closure, was not visible. The relatively short wavelength of the super luminescent diode (820 nm) in the Stratus OCT limits tissue penetration and scattering at the limbus impedes detailed analysis of the angle.

The Visante OCT and the SL-OCT

Two commercially available anterior segment OCT systems, the Visante OCT (Carl Zeiss Meditec) and the SL-OCT (Heidelberg Engineering, GmbH, Dossenheim, Germany), were, respectively, introduced in 2005 and 2006. With a wavelength of 1310 nm, both instruments showed an improvement of tissue penetration through the sclera (Figure 1c and d). The instrument specifications are similar between the two OCT systems (Table 1). Both OCTs are capable of imaging the anterior segment with dimensions of 15–16 mm in width and

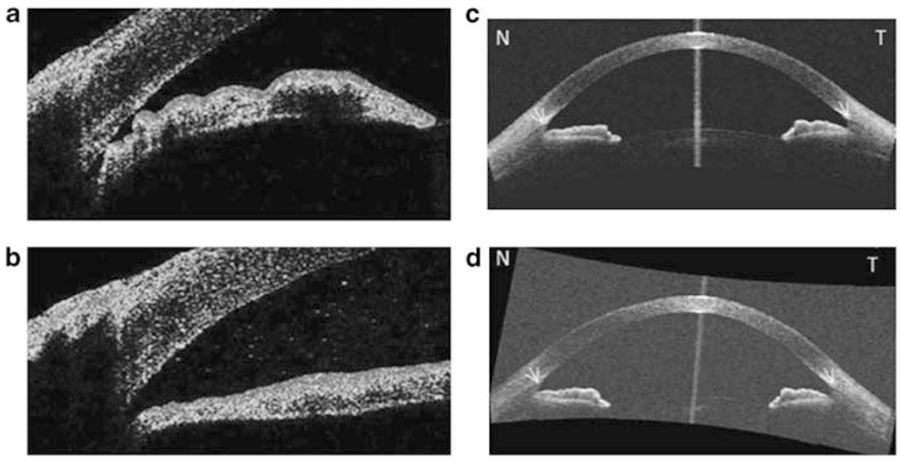

Figure 1 Imaging of the anterior chamber angle with the Stratus OCT (Carl Zeiss Meditec) in an eye with primary angle closure before (a) and right after (b) laser iridotomy. The resulting anterior chamber inflammation after laser iridotomy can be visualized as scattering reflective signals. Although the configuration of the iris and the angle can be examined with the Stratus OCT, the scleral spur could not be detected. With the advent of the anterior segment OCT, visualization of the scleral spur is improved. Examples of clear appearance of the scleral spur in the Visante OCT (Carl Zeiss Meditec; c) and the SL-OCT (Heidelberg Engineering, GmbH; d) images are illustrated (N, nasal; T, temporal). Arrows indicate the locations of the scleral spur. (Modified from Figure 1 in Leung *et al*[3] and Figure 1 in Leung *et al*.[17])

Table 1 Comparison of commercially available OCT systems for anterior chamber angle imaging[5]

	Stratus OCT	*Visante OCT*	*SL-OCT*	*RTVue FD-OCT*	*Cirrus HD-OCT*	*CASIA OCT*
Manufacturer	Carl Zeiss Meditec	Carl Zeiss Meditec	Heidelberg Engineering	Optovue	Carl Zeiss Meditec	Tomey
Year Available	2002	2005	2006	2006	2007	2008
Light Source	Superluminescent Diode 820 nm	Superluminescent Diode 1310 nm	Superluminescent Diode 1310 nm	Superluminescent Diode 840 nm	Superluminescent Diode 840 nm	Swept-source laser 1310 nm
Axial Resolution	10 μm	18 μm	$<$25 μm	5 μm	5 μm	$<$10 μm
Scan Size	6 mm (width) $\times$ 2 mm (depth)	16 mm $\times$ 6 mm	15 mm $\times$ 7 mm	2 mm $\times$ 2 mm (CAM-S) 6 mm $\times$ 2 mm (CAM-L)	3 mm $\times$ 1 mm	16 mm $\times$ 6 mm (low resolution) 8 mm $\times$ 4 mm (high resolution)
Scan Speed	400 A-scans per s	2000 A-scans per s	200 A-scans per s	26 000 A-scans per s	27 000 A-scans per s	30 000 A-scans per s
Fixation Target for Anterior Chamber Angle Imaging	External	Internal and External	External	External	External	Internal and External

Abbreviations: CAM-S, Cornea-Anterior Module Short; CAM-L, Cornea-Anterior Module Long; OCT, optical coherence tomography

6–7 mm in depth and an axial resolution of approximately 18–25 μm. A major difference between the two devices is their scan speed, which is 2000 A-scans per s for Visante OCT, and 200 A-scans per s for SL-OCT. With a line scan of 256 and 215 A-scans, each image frame takes 0.13 and 1.08 s for Visante OCT and SL-OCT, respectively. Another difference is that the Visante OCT has an internal fixation target to adjust for subject's refraction. Correction of refractive error is essential to minimize the variability of pupil size and lens position secondary to accommodation of the eye on measurement of the angle.

Visibility of the scleral spur in anterior segment OCT imaging

Precise location of the scleral spur is a pre-requisite for reliable measurement of the angle. Parameters including the angle-opening distance (AOD), trabecular iris angle (TIA), angle recess area (ARA), and trabecular iris space area (TISA) have been widely adopted to measure the angle dimensions and all of them are measured with reference to the scleral spur (Figure 2).[7,8] However, the scleral spur may not always be visible even with the anterior segment OCT. In a clinic-based study, including 502 participants aged 50 years or older, Sakata *et al*[9] showed the scleral spur was detected in 72% of the Visante OCT images and that the superior and inferior quadrants were less detectable compared with the nasal and temporal quadrants. Using an ordinal scale to grade the visibility of the scleral spur (2 = clear visibility, 1 = moderate visibility, 0 = not detectable) at the 12 clock hours imaged by the Visante OCT, Liu *et al*[10] showed that the inferior quadrant at 6 o'clock had the worst visibility of the scleral spur (mean scleral spur visibility score = 1.05 ± 0.49), whereas the scleral spur was best visualized in the nasal quadrant at 3 o'clock (mean scleral spur visibility score = 1.66 ± 0.46). Methods for measurement of the angle independent of the scleral spur have been proposed. Leung *et al*[11] investigated an automated edge detection algorithm to identify the outlining boundaries of the iris and the scleral-corneal junction at the anterior chamber angle. By fitting the scleral-corneal junction and the iris surface with two regression lines, the angle dimension can be measured. This algorithm, however, may not work well in eyes with a deep angle recess. With the advent of spectral-domain OCT, the angle structures can be examined even greater detail. Schwalbe's line and Schlemm's canal can now be detected with spectral-domain OCT (Figure 3).[12] These structures could serve as useful landmarks to quantify the angle.

Reliability of anterior segment OCT for measurement of the angle

The anterior chamber angle can be outlined cross-sectionally by the junction formed by the scleral-corneal junction, the ciliary body and the peripheral iris. As the configurations of iris and ciliary body vary with lighting condition and accommodation of the eye, the dimensions of the angle can only be measured reproducibly after these covariates have been adjusted. Imaging the anterior chamber angle in the dark is critical to detect angle closure. It has been shown that the angle width is inversely proportional to the pupil size and that the diagnosis of angle-closure could be missed if assessment is not performed in the dark.[13] Likewise, changes in pupil size and lens position during accommodation of the eye can also influence the evaluation of the angle.

Previous studies have shown good repeatability and reproducibility for measurement of AOD, TISA, ARA, and TIA with anterior segment OCT.[14–18] With the lighting condition standardized and the refractive error corrected using an internal fixation target, the intra-session coefficient of variation of the angle width measured with the Visante OCT was $\leq 7\%$ and the inter-session coefficient variation was $\leq 10\%$.[15] The SL-OCT

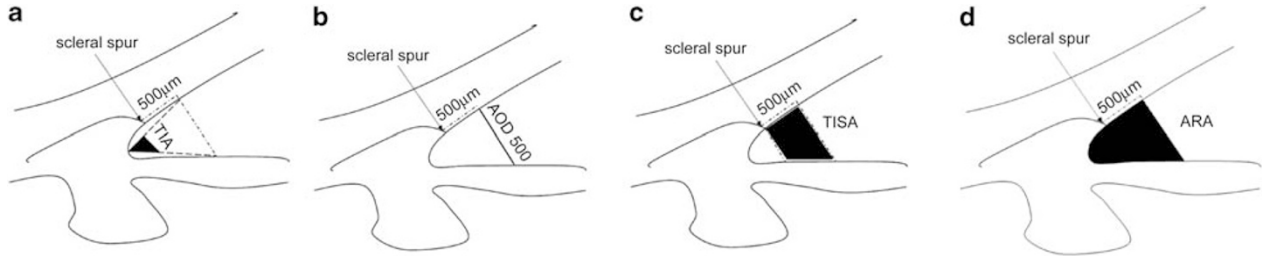

Figure 2 Measurement of trabecular iris angle (TIA; a), angle-opening distance (AOD; b), trabecular iris space area (TISA; c), and angle recess area (ARA; d). TIA 500 is defined as an angle measured with the apex in the iris recess and the arms of the angle passing through a point on the trabecular meshwork 500 μm from the scleral spur and the point on the iris perpendicularly. AOD 500 is calculated as the perpendicular distance measured from the trabecular meshwork at 500 μm anterior to the scleral spur to the anterior iris surface. The TISA 500 is an area bounded anteriorly by the AOD 500; posteriorly by a line drawn from the scleral spur perpendicular to the plane of the inner scleral wall to the opposing iris; superiorly by the inner corneoscleral wall; and inferiorly by the iris surface. ARA 500 is the area of the angle recess bounded anteriorly by the AOD 500. (Modified from Figure 2 in Leung *et al*.[17])

was equally reliable for measurement of the angles. In a study comparing angle measurements between Visante OCT and SL-OCT, the inter-observer coefficient of variation ranged between 4.4 and 7.8%, and between 4.9 and 7.0%, respectively.[17] Nevertheless, the measurement agreement for the two instruments is poor. The spans of 95% limits of agreement of the nasal/temporal angle measurements between the instruments were 437/531 μm, 0.174/0.186 mm^2, and 25.3/28.0° for AOD, TISA, and TIA, respectively.[17]

The spectral-domain OCT

The basic working principle of spectral-domain OCT is similar to time-domain OCT.[19,20] Both systems measure the echo time delay of backscattered light signals via an interferometer. In time-domain OCT, the depth information of the retina is collected as a function of time by moving the reference mirror. The reference mirror in spectral domain OCT, in contrast, is stationary. The light spectrum from the interferometer is detected by a spectrometer. The interference spectrum data is then fourier transformed to generate axial measurements. For this reason, spectral-domain OCT has a much faster scan speed (at least 20 000 A-scans per s) compared with time-domain OCT.

The use of spectral-domain OCT for anterior segment imaging was first described by Radhakrishnan *et al* in 2001.[19] Using a semiconductor optical amplifier light source at a wavelength of 1310 nm, they imaged the anterior segment at a rate of 4–16 frames per s with an axial resolution of 8 μm. Except for the ciliary body, the angle configuration and the scleral spur were clearly visible. Although at least eight commercially available spectral-domain OCT models have been introduced for imaging the optic disc and the macula since 2006, only a few are equipped with additional lens system for anterior segment imaging. By attaching the cornea-anterior module (CAM), the RTVue FD-OCT (Optovue, Fremont, CA, USA) can take an image with dimensions of 6 × 2 mm (CAM-L) or 2 × 2 mm (CAM-S) at the angle (Figure 3a). CAM-L has a lower magnification but a wider field of view compared with CAM-S. The Cirrus HD-OCT (Carl Zeiss Meditec) also allows anterior segment imaging with the built-in 60-diopter aspheric lens. The 'anterior segment five-line raster' is the preferred scan protocol for the angle. The lines are 3 mm in width and covering 1 mm in depth by default (Figure 3b). Using a superluminescent diode laser wavelength of 840 nm in both Cirrus HD-OCT and RTvue FD-OCT, the scleral spur may not be clearly visible although it is possible to identify the Schwalbe's line in most cases (Figure 3a and b). Wong *et al*[12] showed that the Cirrus HD-OCT was capable of detecting the scleral spur in 78.9% and the Schawbles' line in 93.3% of quadrants in 45 individuals (a total of 90 nasal and temporal quadrants) recruited from a glaucoma clinic. As the current software of the RTVue FD-OCT (ver. 4.0) and Cirrus HD-OCT (ver. 5.1) does not adjust for refraction at the air-cornea and cornea-aqueous interfaces (dewarping), imaging should be performed in a direction perpendicular to the limbus to minimize the effect of image distortion. Wylêgała *et al*[21] compared RTVue FD-OCT and Visante OCT for measurement of TIA and AOD in 30 normal volunteers, and did not find any significant differences between the instruments. The

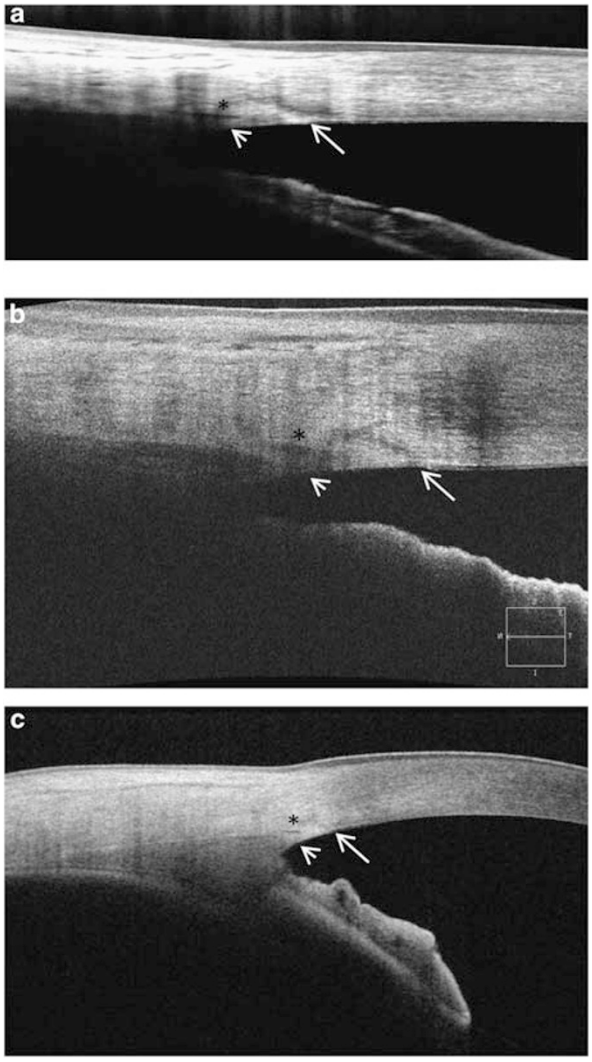

Figure 3 An open anterior chamber angle imaged by the RTVue FD-OCT (2 × 2 mm) (Optovue; a), Cirrus HD-OCT (3 × 1 mm) (Carl Zeiss Meditec; b) and the CASIA OCT (8 × 4 mm) (Tomey; c). Multiple B-scan averaging was performed in RTVue FD-OCT (16 B-scans) and CASIA OCT (3 B-scans). Schwalbe's line-long arrow, scleral spur-short arrow, Schlemm's canal-*.

measurement repeatability and reproducibility of RTVue FD-OCT and Cirrus HD-OCT has not been reported. With a poorer visibility of the scleral spur, the measurement reliability for AOD, TIA, TISA, and ARA might be inferior compared with Visante OCT and SL-OCT. New parameters measured with reference to the Schawbles' line may be more useful to quantify the angle dimensions with these devices.[22]

The swept-source OCT

The swept-source OCT is a form of fourier-domain OCT. Instead of using a spectrometer as in spectral-domain OCT, swept-source OCT uses a monochromatic tunable fast scanning laser source and a photodetector to detect wavelength-resolved interference signal.[23,24] The CASIA OCT (Tomey, Nagoya, Japan) is a commercially available swept-source OCT designed specifically for anterior segment imaging. The wavelength of the swept-source laser is 1310 nm. The scan dimensions are up to 16 mm (width) $\times$ 16 mm (length) $\times$ 6 mm (depth). With a scan speed of 30 000 A-scans per s, it is feasible to collect a series of 64 radial scans across the whole anterior chamber in 1.2 s. With reconstruction of individual image frames, a three-dimensional display of the iris and the anterior chamber angle can be generated (Figure 4).

An advantage of the CASIA OCT is the ability to visualize both the scleral spur and the Schwalbe's line in high-resolution scan mode (Figure 3c). These landmarks represent the boundaries of the trabecular meshwork. Being able to detect the location and measure the dimension of trabecular meshwork may improve the precision of angle measurements and detection of angle closure. The current definitions of angle parameters are made with an assumption that the trabecular meshwork can be found at a distance approximately 500–750 μm away from the scleral spur. This assumption has not been validated. The measurement of trabecular meshwork distance (the distance between the scleral spur and the Schwalbe's line) in relation to the peripheral iris might provide a more reliable approach to quantify the angle.

The applications of OCT for investigation of primary angle closure

OCT imaging has improved the diagnostic performance to detect angle closure. Defining a closed anterior chamber angle as the presence of any contact between the iris and angle wall anterior to the scleral spur, Sakata *et al*[25] showed the Visante OCT detected a closed angle in at least one-quadrant in 59% of the eyes but only 33% by gonioscopy in a community clinic. In all, 71% of cases with closed angles on OCT but open angles by gonioscopy had a short irido-angle contact. The higher proportion of quadrants identified as closed angles on OCT imaging is likely related to the better visualization of the peripheral iris in contact with the trabecular meshwork. Half of the cases with open angles on OCT but closed angles by gonioscopy were found to have a steep iris profile. A false impression of angle closure may result in these eyes by gonioscopy and tilting of the goniolens often is needed to maximize the view of the angles.

OCT imaging can provide mechanistic insights into the pathophysiology of angle closure. The change from a forward bowing to a flattening configuration of the iris after laser iridotomy in eyes with angle closure demonstrates the relief of relative pupillary block and elimination of pressure gradient between the anterior and posterior chambers.[3–6] Widening of the angles has been consistently reported after lens extraction signifying the role of aging lens in contributing to angle closure and

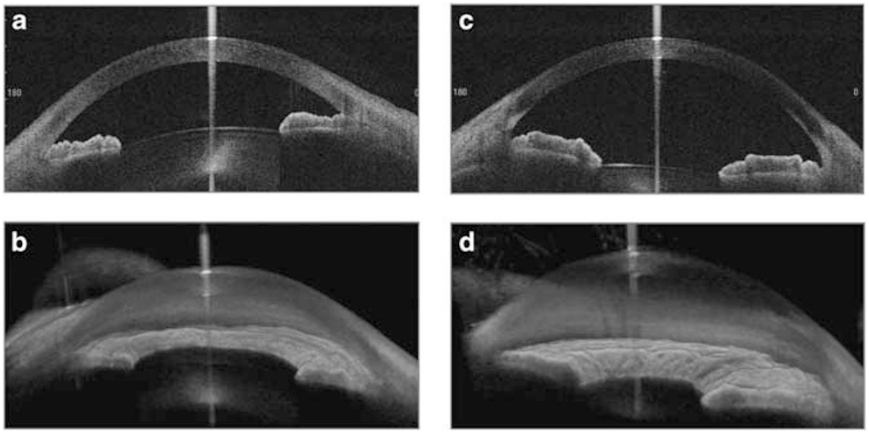

Figure 4 The CASIA OCT (Tomey) is a swept-source OCT with a scan-speed of 30 000 A scans per s. The whole anterior segment can be radially imaged in 64 cross-sections in 1.2 s. A closed angle (a, b) and an open angle (c, d) in cross-section (a, c) and in three-dimensional display (b, d) are illustrated.

supporting lens extraction as a treatment option in management of primary angle closure glaucoma.[26–29]

The measurement of the scleral spur to scleral spur distance with OCT, or the anterior chamber width, has been recently shown to be a risk factor of angle closure.[30] Leung *et al*[31] compared the anterior chamber width, anterior chamber depth, iris thickness, and angle width measured with an anterior segment OCT between Chinese and Caucasian eyes. In agreement with the finding from an epidemiology study,[32] the axial length was not significantly different between the two ethnic groups. More important, the anterior chamber width was found to be shorter in Chinese than in Caucasian eyes even after adjustment of the anterior chamber depth. In other words, the iris-lens diaphragm is more anteriorly located in Chinese. This finding might explain in part the ethnic differences in development of primary angle closure and angle closure glaucoma.

In addition to the anterior chamber width, measurement of the iris has also shown to be important in determining the risk of angle closure.[33–37] Aptel and Denis[34] estimated the iris volume by capturing four cross-sectional images of the anterior segment at 45°-intervals. They showed that iris volume increased from $\sim$45 mm^3 to 50 mm^3 after pharmacologic mydriasis in the fellow non-attacked eyes of patients with history of acute primary angle closure. In contrast, in normal eyes with open-angles, iris volume decreased from $\sim$44 mm^3 to 38 mm^3 after pupil dilation. It has been proposed that differences in iris connective tissue and permeability of the iris stroma to aqueous may account for the differences in volume change in eyes with closed angles and open angles.[38] The expansion in iris with dilation may block aqueous drainage at the angle and predispose to angle closure. Wang *et al*[36] measured iris curvature, iris area, and iris thickness with the Visante OCT and showed that these parameters were independently associated with narrow angles. Cheung *et al* studied the dynamic changes of iris configuration with real-time video capture using the Visante OCT. They found the iris in eyes with narrow or closed angles consistently remained in an anteriorly convex configuration in both light and dark conditions and that the iris curvature is an important determinant of the angle width. With the advent of the spectral-domain and swept-source OCT imaging systems, iris volume and iris configuration can be quantified in more details. This information would be valuable in studying iris dynamics in relation to development of primary angle closure.

Summary

Ultrahigh speed 1050 nm swept-source fourier-domain OCT for anterior segment imaging is under development and imaging at a speed of 100 000 to 400 000 axial scans per s has been recently demonstrated.[39] With the development of high-resolution and high-speed OCT imaging systems, angle structures including the scleral spur, Schwalbe's line and Schlemm's canal can be examined. The iris profiles and the angle configurations can be visualized three dimensionally and evaluated for 360°. It is conceivable that OCT imaging of the anterior segment could improve detection of angle closure and provide mechanistic insights into the pathophysiology of acute primary angle closure and angle closure glaucoma.

Conflict of interest

The authors declare no conflict of interest.

Acknowledgements

CL has received research support from Carl Zeiss Meditec, Optovue, and Tomey, and honorarium from Carl Zeiss Meditec for conference presentation.
RW is a consultant to Carl Zeiss Meditec. RW has received research support from Carl Zeiss Meditec and Optovue.

References

1 Huang D, Swanson EA, Lin CP, Schuman JS, Stinson WG, Chang W *et al*. Optical coherence tomography. *Science* 1991; **254**: 1178–1181.
2 Izatt JA, Hee MR, Swanson EA, Lin CP, Huang D, Schuman JS *et al*. Micrometer-scale resolution imaging of the anterior eye *in vivo* with optical coherence tomography. *Arch Ophthalmol* 1994; **112**: 1584–1589.
3 Leung CK, Chan WM, Ko CY, Chui SI, Woo J, Tsang MK *et al*. Visualization of anterior chamber angle dynamics using optical coherence tomography. *Ophthalmology* 2005; **112**: 980–984.
4 Ang GS, Wells AP. Changes in Caucasian eyes after laser peripheral iridotomy: an anterior segment optical coherence tomography study. *Clin Experiment Ophthalmol* 2010; **38**: 778–785.
5 See JL, Chew PT, Smith SD, Nolan WP, Chan YH, Huang D *et al*. Changes in anterior segment morphology in response to illumination and after laser iridotomy in Asian eyes: an anterior segment OCT study. *Br J Ophthalmol* 2007; **91**: 1485–1489.
6 Memarzadeh F, Li Y, Chopra V, Varma R, Francis BA, Huang D. Anterior segment optical coherence tomography for imaging the anterior chamber after laser peripheral iridotomy. *Am J Ophthalmol* 2007; **143**: 877–879.
7 Pavlin CJ, Harasiewicz K, Foster FS. Ultrasound biomicroscopy of anterior segment structures in normal and glaucomatous eyes. *Am J Ophthalmol* 1992; **113**: 381–389.
8 Radhakrishnan S, Goldsmith J, Huang D, Westphal V, Dueker DK, Rollins AM *et al*. Comparison of optical coherence tomography and ultrasound biomicroscopy for detection of narrow anterior chamber angles. *Arch Ophthalmol* 2005; **123**: 1053–1059.
9 Sakata LM, Lavanya R, Friedman DS, Aung HT, Seah SK, Foster PJ *et al*. Assessment of the scleral spur in anterior

segment optical coherence tomography images. *Arch Ophthalmol* 2008; **126**: 181–185.
10 Liu S, Li H, Dorairaj S, Cheung CY, Rousso J, Liebmann J *et al.* Assessment of scleral spur visibility with anterior segment optical coherence tomography. *J Glaucoma* 2010; **19**: 132–135.
11 Leung CK, Yung WH, Yiu CK, Lam SW, Leung DY, Tse RK *et al.* Novel approach for anterior chamber angle analysis: anterior chamber angle detection with edge measurement and identification algorithm (ACADEMIA). *Arch Ophthalmol* 2006; **124**: 1395–1401.
12 Wong HT, Lim MC, Sakata LM, Aung HT, Amerasinghe N, Friedman DS *et al.* High-definition optical coherence tomography imaging of the iridocorneal angle of the eye. *Arch Ophthalmol* 2009; **127**: 256–260.
13 Leung CK, Cheung CY, Li H, Dorairaj S, Yiu CK, Wong AL *et al.* Dynamic analysis of dark-light changes of the anterior chamber angle with anterior segment OCT. *Invest Ophthalmol Vis Sci* 2007; **48**: 4116–4122.
14 Müller M, Dahmen G, Pörksen E, Geerling G, Laqua H, Ziegler A *et al.* Anterior chamber angle measurement with optical coherence tomography: intraobserver and interobserver variability. *J Cataract Refract Surg* 2006; **32**: 1803–1808.
15 Li H, Leung CK, Cheung CY, Wong L, Pang CP, Weinreb RN *et al.* Repeatability and reproducibility of anterior chamber angle measurement with anterior segment optical coherence tomography. *Br J Ophthalmol* 2007; **91**: 1490–1492.
16 Radhakrishnan S, See J, Smith SD, Nolan WP, Ce Z, Friedman DS *et al.* Reproducibility of anterior chamber angle measurements obtained with anterior segment optical coherence tomography. *Invest Ophthalmol Vis Sci* 2007; **48**: 3683–3688.
17 Leung CK, Li H, Weinreb RN, Liu J, Cheung CY, Lai RY *et al.* Anterior chamber angle measurement with anterior segment optical coherence tomography: a comparison between slit lamp OCT and Visante OCT. *Invest Ophthalmol Vis Sci* 2008; **49**: 3469–3474.
18 Tan AN, Sauren LD, de Brabander J, Berendschot TT, Lima Passos V, Webers CA *et al.* Reproducibility of anterior chamber angle measurements with anterior segment optical coherence tomography. *Invest Ophthalmol Vis Sci* 2010 (in press).
19 Radhakrishnan S, Rollins AM, Roth JE, Yazdanfar S, Westphal V, Bardenstein DS *et al.* Real-time optical coherence tomography of the anterior segment at 1310 nm. *Arch Ophthalmol* 2001; **119**: 1179–1185.
20 Nassif N, Cense B, Park BH, Yun SH, Chen TC, Bouma BE *et al. In vivo* human retinal imaging by ultrahigh-speed spectral-domain optical coherence tomography. *Opt Lett* 2004; **29**: 480–482.
21 Wylegał E, Teper S, Nowińska AK, Milka M, Dobrowolski D. Anterior segment imaging: fourier-domain optical coherence tomography versus time-domain optical coherence tomography. *J Cataract Refract Surg* 2009; **35**: 1410–1414.
22 Aung T, Zheng C, Tun TA, Kumar RS, Wong TY, Cheung CY. Novel anterior chamber angle measurements with high definition optical coherence tomography using the Schwalbe's line as the landmark. *ARVO Meet Abstracts* 2010; **51**: 3855.
23 Yun S, Tearney G, de Boer J, Iftimia N, Bouma B. High-speed optical frequency-domain imaging. *Opt Express* 2003; **11**: 2953–2963.
24 Yasuno Y, Madjarova VD, Makita S, Akiba M, Morosawa A, Chong C *et al.* Three-dimensional and high-speed swept-source optical coherence tomography for *in vivo* investigation of human anterior eye segments. *Opt Express* 2005; **13**: 10652–10664.
25 Sakata LM, Lavanya R, Friedman DS, Aung HT, Gao H, Kumar RS *et al.* Comparison of gonioscopy and anterior segment ocular coherence tomography in detecting angle closure in different quadrants of the anterior chamber angle. *Ophthalmology* 2008; **115**: 769–774.
26 Memarzadeh F, Tang M, Li Y, Chopra V, Francis BA, Huang D. Optical coherence tomography assessment of angle anatomy changes after cataract surgery. *Am J Ophthalmol* 2007; **144**: 464–465.
27 Nolan WP, See JL, Aung T, Friedman DS, Chan YH, Smith SD *et al.* Changes in angle configuration after phacoemulsification measured by anterior segment optical coherence tomography. *J Glaucoma* 2008; **17**: 455–459.
28 Kucumen RB, Yenerel NM, Gorgun E, Kulacoglu DN, Dinc UA, Alimgil ML. Anterior segment optical coherence tomography measurement of anterior chamber depth and angle changes after phacoemulsification and intraocular lens implantation. *J Cataract Refract Surg* 2008; **34**: 1694–1698.
29 Tai MC, Chien KH, Lu DW, Chen JT. Angle changes before and after cataract surgery assessed by Fourier-domain anterior segment optical coherence tomography. *J Cataract Refract Surg* 2010; **36**: 1758–1762.
30 Nongpiur ME, Sakata LM, Friedman DS, He M, Chan YH, Lavanya R *et al.* Novel association of smaller anterior chamber width with angle closure in Singaporeans. *Ophthalmology* 2010; **117**: 1967–1973.
31 Leung CK, Palmiero PM, Weinreb RN, Li H, Sbeity Z, Dorairaj S *et al.* Comparisons of anterior segment biometry between Chinese and Caucasians using anterior segment optical coherence tomography. *Br J Ophthalmol* 2010; **94**: 1184–1189.
32 Congdon NG, Youlin Q, Quigley H, Hung PT, Wang TH, Ho TC *et al.* Biometry and primary angle-closure glaucoma among Chinese, White, and Black populations. *Ophthalmology* 1997; **104**: 1489–1495.
33 Quigley HA, Silver DM, Friedman DS, He M, Plyler RJ, Eberhart CG *et al.* Iris cross-sectional area decreases with pupil dilation and its dynamic behavior is a risk factor in angle closure. *J Glaucoma* 2009; **18**: 173–179.
34 Aptel F, Denis P. Optical coherence tomography quantitative analysis of iris volume changes after pharmacologic mydriasis. *Ophthalmology* 2010; **117**: 3–10.
35 Wang BS, Narayanaswamy A, Amerasinghe N, Zheng C, He M, Chan YH *et al.* Increased iris thickness and association with primary angle closure glaucoma. *Br J Ophthalmol* 2010; **95**(1): 46–50.
36 Wang B, Sakata LM, Friedman DS, Chan YH, He M, Lavanya R *et al.* Quantitative iris parameters and association with narrow angles. *Ophthalmology* 2010; **117**: 11–17.
37 Cheung CY, Liu S, Weinreb RN, Liu J, Li H, Leung DY *et al.* Dynamic analysis of iris configuration with anterior segment optical coherence tomography. *Invest Ophthalmol Vis Sci* 2010; **51**: 4040–4046.
38 Quigley HA. Angle-closure glaucoma-simpler answers to complex mechanisms: LXVI Edward Jackson Memorial Lecture. *Am J Ophthalmol* 2009; **148**: 657–669.
39 Potsaid B, Baumann B, Huang D, Barry S, Cable AE, Schuman JS *et al.* Ultrahigh speed 1050 nm swept source/fourier domain OCT retinal and anterior segment imaging at 100 000 to 400 000 axial scans per second. *Opt Express* 2010; **18**: 20029–20048.